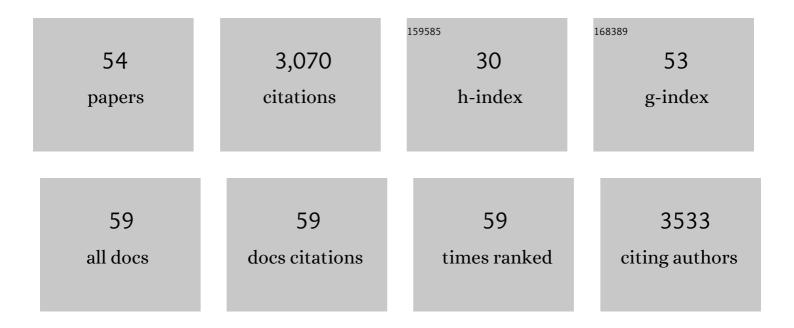
## Eric C Tyrode

List of Publications by Year in descending order

Source: https://exaly.com/author-pdf/7765409/publications.pdf Version: 2024-02-01



FRIC C TYRODE

#	Article	IF	CITATIONS
1	Water at Interfaces. Chemical Reviews, 2016, 116, 7698-7726.	47.7	536
2	Adsorption of CTAB on Hydrophilic Silica Studied by Linear and Nonlinear Optical Spectroscopy. Journal of the American Chemical Society, 2008, 130, 17434-17445.	13.7	223
3	Current Phenomenological Know-How and Modeling of Emulsion Inversion. Industrial & Engineering Chemistry Research, 2000, 39, 2665-2676.	3.7	137
4	Hydration State of Nonionic Surfactant Monolayers at the Liquid/Vapor Interface:Â Structure Determination by Vibrational Sum Frequency Spectroscopy. Journal of the American Chemical Society, 2005, 127, 16848-16859.	13.7	131
5	Hydrophobic Surfaces: Topography Effects on Wetting by Supercooled Water and Freezing Delay. Journal of Physical Chemistry C, 2013, 117, 21752-21762.	3.1	113
6	The elusive silica/water interface: isolated silanols under water as revealed by vibrational sum frequency spectroscopy. Physical Chemistry Chemical Physics, 2017, 19, 10343-10349.	2.8	111
7	A Vibrational Sum Frequency Spectroscopy Study of the Liquidâ^'Gas Interface of Acetic Acidâ^'Water Mixtures:Â 1. Surface Speciation. Journal of Physical Chemistry B, 2005, 109, 321-328.	2.6	97
8	Simultaneous Conductivity and Viscosity Measurements as a Technique To Track Emulsion Inversion by the Phase-Inversion-Temperature Method. Langmuir, 2004, 20, 2134-2140.	3.5	96
9	A Vibrational Sum Frequency Spectroscopy Study of the Liquidâ^'Gas Interface of Acetic Acidâ^'Water Mixtures:Â 2. Orientation Analysis. Journal of Physical Chemistry B, 2005, 109, 329-341.	2.6	90
10	A Comparative Study of the CD and CH Stretching Spectral Regions of Typical Surfactants Systems Using VSFS: Orientation Analysis of the Terminal CH <sub>3</sub> and CD <sub>3</sub> Groups. Journal of Physical Chemistry C, 2012, 116, 1080-1091.	3.1	85
11	Water Structure Next to Ordered and Disordered Hydrophobic Silane Monolayers: A Vibrational Sum Frequency Spectroscopy Study. Journal of Physical Chemistry C, 2013, 117, 1780-1790.	3.1	82
12	Phospholipid Monolayers Probed by Vibrational Sum Frequency Spectroscopy: Instability of Unsaturated Phospholipids. Biophysical Journal, 2010, 98, L50-L52.	0.5	74
13	Emulsion Catastrophic Inversion from Abnormal to Normal Morphology. 2. Effect of the Stirring Intensity on the Dynamic Inversion Frontier. Industrial & Engineering Chemistry Research, 2003, 42, 57-61.	3.7	67
14	Study of the adsorption of sodium dodecyl sulfate (SDS) at the air/water interface: targeting the sulfate headgroup using vibrational sum frequency spectroscopy. Physical Chemistry Chemical Physics, 2005, 7, 2635.	2.8	66
15	Emulsion Catastrophic Inversion from Abnormal to Normal Morphology. 1. Effect of the Water-to-Oil Ratio Rate of Change on the Dynamic Inversion Frontier. Industrial & Engineering Chemistry Research, 2003, 42, 50-56.	3.7	65
16	Vibrational Sum Frequency Spectroscopy Studies at Solid/Liquid Interfaces: Influence of the Experimental Geometry in the Spectral Shape and Enhancement. Journal of Physical Chemistry C, 2012, 116, 22893-22903.	3.1	62
17	Structure and Hydration of Poly(ethylene oxide) Surfactants at the Air/Liquid Interface. A Vibrational Sum Frequency Spectroscopy Study. Journal of Physical Chemistry C, 2007, 111, 11642-11652.	3.1	59
18	Emulsion Catastrophic Inversion from Abnormal to Normal Morphology. 4. Following the Emulsion Viscosity during Three Inversion Protocols and Extending the Critical Dispersed-Phase Concept. Industrial & Engineering Chemistry Research, 2005, 44, 67-74.	3.7	58

Eric C Tyrode

#	Article	IF	CITATIONS
19	Emulsion Catastrophic Inversion from Abnormal to Normal Morphology. 3. Conditions for Triggering the Dynamic Inversion and Application to Industrial Processes. Industrial & Engineering Chemistry Research, 2003, 42, 4311-4318.	3.7	55
20	3D titania photonic crystals replicated from gyroid structures in butterfly wing scales: approaching full band gaps at visible wavelengths. RSC Advances, 2013, 3, 3109.	3.6	54
21	Molecular insight into carboxylic acid–alkali metal cations interactions: reversed affinities and ion-pair formation revealed by non-linear optics and simulations. Physical Chemistry Chemical Physics, 2019, 21, 11329-11344.	2.8	50
22	Probing Charged Aqueous Interfaces Near Critical Angles: Effect of Varying Coherence Length. Journal of Physical Chemistry C, 2019, 123, 16911-16920.	3.1	49
23	On the colour of wing scales in butterflies: iridescence and preferred orientation of single gyroid photonic crystals. Interface Focus, 2017, 7, 20160154.	3.0	48
24	Active corrosion protection by conductive composites of polyaniline in a UV-cured polyester acrylate coating. Progress in Organic Coatings, 2016, 90, 154-162.	3.9	43
25	The premolten layer of ice next to a hydrophilic solid surface: correlating adhesion with molecular properties. Physical Chemistry Chemical Physics, 2017, 19, 305-317.	2.8	40
26	Charging of Carboxylic Acid Monolayers with Monovalent Ions at Low Ionic Strengths: Molecular Insight Revealed by Vibrational Sum Frequency Spectroscopy. Journal of Physical Chemistry C, 2018, 122, 28775-28786.	3.1	40
27	Preferential Adsorption of Amino-Terminated Silane in a Binary Mixed Self-Assembled Monolayer. Langmuir, 2011, 27, 5420-5426.	3.5	39
28	A Study of the Adsorption of Ammonium Perfluorononanoate at the Airâ^'Liquid Interface by Vibrational Sum-Frequency Spectroscopy. Journal of Physical Chemistry C, 2007, 111, 316-329.	3.1	37
29	Surface Grafted Chitosan Gels. Part II. Gel Formation and Characterization. Langmuir, 2014, 30, 8878-8888.	3.5	35
30	Vibrational Sum Frequency Spectroscopy Study of the Liquid/Vapor Interface of Formic Acid/Water Solutions. Journal of Physical Chemistry C, 2009, 113, 13209-13218.	3.1	31
31	Silica Surface Charge Enhancement at Elevated Temperatures Revealed by Interfacial Water Signals. Journal of the American Chemical Society, 2020, 142, 669-673.	13.7	31
32	Influence of the Stirrer Initial Position on Emulsion Morphology. Making Use of the Local Water-to-Oil Ratio Concept for Formulation Engineering Purpose. Industrial & Engineering Chemistry Research, 2001, 40, 4808-4814.	3.7	28
33	Single- and Two-Step Emulsification To Prepare a Persistent Multiple Emulsion with a Surfactantâ^'Polymer Mixture. Industrial & Engineering Chemistry Research, 2003, 42, 3982-3988.	3.7	26
34	Surface Grafted Chitosan Gels. Part I. Molecular Insight into the Formation of Chitosan and Poly(acrylic acid) Multilayers. Langmuir, 2014, 30, 8866-8877.	3.5	26
35	Foamability and foam stability at high pressures and temperatures. I. Instrument validation. Review of Scientific Instruments, 2003, 74, 2925-2932.	1.3	25
36	Molecular Structure upon Compression and Stability toward Oxidation of Langmuir Films of Unsaturated Fatty Acids: A Vibrational Sum Frequency Spectroscopy Study. Langmuir, 2010, 26, 14024-14031.	3.5	25

Eric C Tyrode

#	Article	IF	CITATIONS
37	Neat Water–Vapor Interface: Proton Continuum and the Nonresonant Background. Journal of Physical Chemistry Letters, 2018, 9, 6744-6749.	4.6	25
38	Atmospheric Corrosion of Zinc by Organic Constituents. Journal of the Electrochemical Society, 2006, 153, B113.	2.9	23
39	Structure of the Silica/Divalent Electrolyte Interface: Molecular Insight into Charge Inversion with Increasing pH. Journal of Physical Chemistry C, 2020, 124, 26973-26981.	3.1	23
40	Interactions of Na <sup>+</sup> Cations with a Highly Charged Fatty Acid Langmuir Monolayer: Molecular Description of the Phase Transition. Journal of Physical Chemistry C, 2019, 123, 23037-23048.	3.1	20
41	Soluble Monolayers ofn-Decyl Glucopyranoside andn-Decyl Maltopyranoside. Phase Changes in the Gaseous to the Liquid-Expanded Range. Langmuir, 2005, 21, 305-315.	3.5	18
42	Identifying Eigen-like hydrated protons at negatively charged interfaces. Nature Communications, 2020, 11, 493.	12.8	17
43	La3+ and Y3+ interactions with the carboxylic acid moiety at the liquid/vapor interface: Identification of binding complexes, charge reversal, and detection limits. Journal of Colloid and Interface Science, 2022, 608, 2169-2180.	9.4	17
44	Temperature-Dependent Deicing Properties of Electrostatically Anchored Branched Brush Layers of Poly(ethylene oxide). Langmuir, 2016, 32, 4194-4202.	3.5	15
45	The Jones–Ray Effect Is Not Caused by Surface-Active Impurities. Journal of Physical Chemistry Letters, 2018, 9, 6739-6743.	4.6	15
46	Charge regulation and energy dissipation while compressing and sliding a cross-linked chitosan hydrogel layer. Journal of Colloid and Interface Science, 2015, 443, 162-169.	9.4	12
47	Molecular Structural Information of the Atmospheric Corrosion of Zinc Studied by Vibrational Spectroscopy Techniques. Journal of the Electrochemical Society, 2010, 157, C357.	2.9	11
48	Self-assembly of long chain fatty acids: effect of a methyl branch. Physical Chemistry Chemical Physics, 2014, 16, 17869-17882.	2.8	9
49	Anion Specific Effects at Negatively Charged Interfaces: Influence of Cl <sup>–</sup> , Br <sup>–</sup> , I <sup>–</sup> , and SCN <sup>–</sup> on the Interactions of Na <sup>+</sup> with the Carboxylic Acid Moiety. Journal of Physical Chemistry B, 2021, 125, 12384-12391.	2.6	9
50	Surfactant-Oil-Water Systems Near the Affinity Inversion. XII: Emulsion Drop Size Versus Formulation and Composition. Journal of Dispersion Science and Technology, 2002, 23, 55-63.	2.4	8
51	The Molecular Surface Structure of Ammonium and Potassium Dinitramide: A Vibrational Sum Frequency Spectroscopy and Quantum Chemical Study. Journal of Physical Chemistry C, 2011, 115, 10588-10596.	3.1	7
52	Cryoporometry in Femtoliter Volumes by Confocal Raman Spectroscopy. Langmuir, 2019, 35, 8823-8828.	3.5	3
53	Molecular Structure and Stability of Phospholipid Monolayers Probed by Vibrational Sum Frequency Spectroscopy (VSFS). Biophysical Journal, 2012, 102, 591a.	0.5	2
54	3-D Chiral Photonic Crystals Replicated from Butterfly Wing Scales. Materials Research Society Symposia Proceedings, 2012, 1389, 1.	0.1	0